PION-^{12}C NUCLEUS OPTICAL POTENTIAL

A.A. Ebrahim, S.A.E. Khallaf

Physics Department, Assiut University, Assiut 71516, Egypt

(Received November 30, 2004)

Elastic and inelastic cross sections for pion scattering on ^{12}C at pion kinetic energy ranging from 50 to 260 MeV are computed using three independent methods of $\pi^{\pm}$-nucleus optical potential, the 3α-particle model of the nucleus, the equivalent local Kisslinger potential, and the Laplacian one. Reasonable fits to the measured values are obtained for ^{12}C without adjusting free parameters. The ability of these methods to account for elastic, inelastic, total, and reaction cross section data are somewhat similar. The Kisslinger-based local potential is the more suitable for describing the elastic and inelastic cross sections of $\pi^{\pm}$-nucleus scattering. It seems that the 3α-particle model of ^{12}C is not useful in the description of pion scattering on ^{12}C at least in the Δ-resonance region.

PACS numbers: 25.80.Dj, 25.80.Ek, 24.10.Eq, 21.60.Ev

1. Introduction

Pion-nucleus scattering at energies from about 100 to 300 MeV can be described in terms of just a simple optical potential which is of the form of the nuclear density multiplied by the elementary pion–nucleon off-shell T-matrix; the first order pion–nucleus distorted wave impulse approximation code DWPI [1]. The success of this first order optical potential can be understood as a consequence of the dominance of the pion–nucleon (3,3) resonance in this energy region, since due to the resonance the optical potential is highly absorptive so that the mean free path of the pion is very small and consequently most of the scattering takes place in the nuclear surface. At the same time, second order corrections to the optical potential necessarily involve the square of the density, so that they are strong only in the interior of the nucleus where the pion never gets the opportunity to enter. If one moves in energy away below the (3,3) resonance, the pion has more chance to sample the interior region of the nucleus and consequently higher order effects will start to appear [2].

The multiple scattering theory leading to the optical potential was first developed by Watson and his collaborators [3], and subsequently in a more complete form by Kerman, McManus and Thaler [4]. Calculations have shown that if various effects are taken into account, then differences between theoretical predictions and experimental data can be much reduced, see *e.g.* Ref. [5].

On the other hand, ^{12}C is a typical nucleus with the α-particle structure. It is considered to consist of three α-particles and these α-particles basically retain the feature of a free α-particle. The α-particle is bounded much more weakly than a nucleon in the ^{12}C nucleus. Local π-nucleus optical potential was constructed based on the α-particle model of the ^{12}C nucleus [6] where the π–α amplitude was directly obtained from fitting the experimental data. It was argued in Ref. [6] that the various effects indicated above would be automatically included to a certain extent in the π–α amplitudes. This simple model gave fairly good results over a wide energy region for π-^{12}C elastic scattering, particularly in the low-energy region [6].

Moreover, two forms of potential are commonly used to describe the pion–nucleus interaction. These two forms are the Kisslinger [7] potential and a Laplacian [8] one. Both contain explicitly terms which originate in the p-wave pion–nucleon interaction which are important near the (3,3) resonance energy. The Kisslinger nonlocal potential [7] is:

$$U_{\rm Kis}(r) = \frac{(\hbar c)^2}{2\omega} \left\{ q(r) + \nabla \cdot \alpha(r) \nabla \right\} , \tag{1}$$

where ω is the total energy of the pion in the center of mass (c.m.) system, the quantities $q(r)$ and $\alpha(r)$ mainly result from the s- and p-waves of the pion–nucleon interaction and they are complex and energy dependent and given in detail in Ref. [9].

Recently, Johnson and Satchler [9] used the Krell–Ericson transformation [10], which leads from the Klein–Gordon equation for pion scattering to a local potential for the transformed wave function, equivalent to the Kisslinger nonlocal potential. This local potential was used to successfully analyze the elastic scattering of $\pi^{\pm}$ from ^{12}C, ^{16}O, ^{28}Si, and ^{40,44,48}Ca in the pion kinetic energy range of 30 to 292 MeV [11]. Elastic and inelastic scattering of positive and negative pions from calcium isotopes and ^{54}Fe were studied [12] using the Kisslinger local potential, together with a zero-range DWBA code. The DWUCK4 code [13] was used to calculate the differential cross section angular distributions for elastically and inelastically scattered pions from these targets. It was concluded that the DWUCK4 code and the local-equivalent Kisslinger potential of Johnson and Satchler are reliable models for pion–nucleus scattering.

The aim of the present work is to calculate the angular distributions of the differential cross sections of the $\pi^{\pm}$ elastically and inelastically scattered to the lowest 2^+ and 3^- states in ^{12}C in the energy range of 50 to 260 MeV, using three independent methods of $\pi^{\pm}$-nucleus optical potential, the 3α-particle model of the nucleus [6], the local-equivalent Kisslinger potential [9], and the Laplacian local potential [8]. The results of the three calculations are compared to the experimental data [14, 15]. The total and reaction cross section for these reactions are calculated and compared to the corresponding ones estimated by others. The methods employed here are described in Section 2, the results and discussion are given in Section 3 and the conclusions are presented in Section 4.

2. Method

Three different forms of the optical potential have been used to study pion–nucleus interactions in the low and resonance regions. In the first form, Li Qing-run [6] has demonstrated that the α-particle model interaction gives a reasonable description of π-^{12}C elastic scattering in the resonance region. The nuclear π-nucleus optical potential in the α-particle model is local and given by [6]:

$$U_{00}(r) \;=\; B_0\, Q_0(r) \;+\; B_2\, Q_2(r) \;+\; B_4\, Q_4(r) \;+\; B_6\, Q_6(r) \;+\; B_8\, Q_8(r)\,, \quad (2)$$

where the expressions for the B's and Q's are given in detail in Ref. [6].

A second form of the pion–nucleus potential is obtained by the Kisslinger local potential [9], in this treatment the transformed potential is local and given by [9]:

$$U_{\mathrm{Loc}}(r) \;=\; \frac{(\hbar c)^2}{2\omega}\left\{\frac{q(r)}{1-\alpha(r)} - \frac{k^2\,\alpha(r)}{1-\alpha(r)} - \frac{\frac{1}{2}\,\nabla^2\,\alpha(r)}{1-\alpha(r)} - \left(\frac{\frac{1}{2}\nabla\,\alpha(r)}{1-\alpha(r)}\right)^2\right\} + \frac{\alpha(r)\,V_{\mathrm{C}} - (V_{\mathrm{C}}^2/2\omega)}{1-\alpha(r)}\,, \quad (3)$$

with $q(r)$ and $\alpha(r)$ the same as for the Kisslinger nonlocal potential, and k the wave number of the pion–nucleon in the center of momentum frame. The first term is nuclear local potential and the second term is the Coulomb correction. Here, V_{C} is the Coulomb potential due to the uniform charge distribution of the target nucleus of radius $R_{\mathrm{C}} = r_{\mathrm{C}}\, A^{1/3}$, A is the target mass number and r_{C}=1.2 fm [12].

A third method is the Laplacian model, where the potential is local and is written as [8]:

$$U_{\rm Lap}(r) = \frac{(\hbar c)^2}{2\omega}\,\left\{q(r) - k^2\,\alpha(r) - \tfrac{1}{2}\nabla^2\,\alpha(r)\right\}\,, \tag{4}$$

$q(r)$ and $\alpha(r)$ are similar to those in Eq. (1).

The first-order parameters b_i and c_i (i = 0,1) for various pion kinetic energies T_π considered here are calculated through the phase shifts, as they are computed in the code of Ref. [16] . These parameters b_i and c_i are then used to generate the complex local potential $\rm U_{Loc}$ using the expressions from Ref. [9]. The same parameters b_i and c_i are also used for calculations in the Laplacian model to compare to the Kisslinger local potential calculations. The second-order parameters B_0 and C_0 which are very important at lower pion energies $T_\pi < 100$ MeV are taken into account here and are taken from Ref. [11].

For inelastic π-nucleus scattering, the radial parts of the hadronic transition potentials used here are as follows [17]:

$$V(r) = -\,\gamma_l\,\frac{dU_{00}(r)\ \text{or}\ dU_{\rm Loc}(r)\ \text{or}\ dU_{\rm Lap}(r)}{dr}\,, \tag{5}$$

where $U_{00}(r)$ is the pion–nucleus optical potential in the α-particle model, $U_{\rm Loc}(r)$ is the local transformed potential, and $U_{\rm Lap}(r)$ is the Laplacian potential. These potentials are those used to fit the corresponding elastic scattering data. In the present work, all other factors are kept the same as in the case of elastic π-^{12}C scattering. When using the Kisslinger local or Laplacian potentials, the transformed wave function used in $\pi-^{12}$C elastic scattering analysis is also employed in the case of inelastic scattering without any changes. For a given transition, we use γ_l to denote the corresponding "deformation lengths" for the $\pi^\pm$ interactions, where $l(=2$ or 3) is the multipolarity.

To differentiate between the above mentioned potentials, the quality of fits to the calculated differential cross sections using these potentials is judged according to the following well known relation:

$$\chi^2 = \sum_{i=1}^{N}\left(\left[\frac{d\sigma_{\rm exp}(\theta_i)}{d\Omega} - \frac{d\sigma_{\rm th}(\theta_i)}{d\Omega}\right]\Big/\,\Delta\left(\frac{d\sigma_{\rm exp}(\theta_i)}{d\Omega}\right)\right)^2\Big/\,N\,. \tag{6}$$

Here N is the number of data points, $d\sigma_{\rm exp}(\theta_i)/d\Omega$ and $d\sigma_{\rm th}(\theta_i)/d\Omega$ are, respectively, the experimental and theoretical differential cross sections and $\Delta(d\sigma_{\rm exp}(\theta_i)/d\Omega)$ is the error in each datum. The χ^2 values obtained in the present work are included in Tables II and IV.

3. Results and discussion

To calculate the cross sections for $\pi^{\pm}$ elastic scattering we have used the α-particle model, the Kisslinger local potential, and the Laplacian potential. The calculated results for ^{12}C involving no free parameters are compared with the experimental cross sections [14, 15] in Figs. 1 and 3. The resulting kinematic and parameter values for the cases studied here are calculated according to equations given in Ref. [17] and are listed in Table I. For elastic and inelastic scattering from ^{12}C, the values of the first- and second-order parameters are of the same values for π^+ and π^- scattering at a certain beam energy. In the present calculations we used the three parameter Fermi shape for the density distributions of nucleons within ^{12}C along with the Ericson–Ericson Lorentz–Lorentz (EELL) parameter ζ=1.0, they were more suitable for $\pi^{\pm}$-nucleus scattering using the Kisslinger local potential [11], in the same energy range considered here.

TABLE I

Kinematic factors for use in a nonrelativistic Schrödinger equation used in the present work with pion kinetic energy T_π. E_L, M_π, k, and p_1 are the effective bombarding energy, effective pion mass, pion wave number, and kinematic transformation factor, respectively.

T_π(MeV)	E_L (MeV)	$M_\pi(u)$	k (fm^{-1})	p_1
50	43.63	0.20189	0.639	1.1825
150	113.30	0.30501	1.254	1.2726
180	132.20	0.33558	1.417	1.2992
220	156.32	0.37543	1.625	1.3345
260	180.66	0.41629	1.833	1.3687

We note that both α-particle model and the Kisslinger local potential model give similar predictions except at large angles. In particular, both models predict two diffraction minima, but the predicted minima are much deeper than those observed. For Laplacian model, there exists a sizable discrepancy in the magnitude and shape of the cross section and the calculated values do not have the energy dependence of the data.

In Fig. 1 the elastic scattering differential cross sections at forward angles and the positions of the minima and the maximum agree well with the calculated values of the Kisslinger local potential but at 260 MeV calculations with the α-particle model and Laplacian potential do not reproduce the depth and height of the structure around the minimum. Calculations using the first-order Kisslinger local potential are in better agreement with the experimental cross sections at the three energies 150, 180, and 260 MeV

(χ^2=2.80-4.63), and α-particle model calculations are in reasonable agreement with data (χ^2=9.13-11.65), while the Laplacian model calculations fail to agree the data at these three energies especially at large angles (χ^2=10.41–14.12). The important difference between the Kisslinger local potential and Laplacian model is the charge effect, in the $U_{\rm Loc}$ potential the (1-α) denominator applies also to the full local term, including the Coulomb term, while $U_{\rm Lap}$ does not have any Coulomb effects other than those explicit in the transformed wave equation.

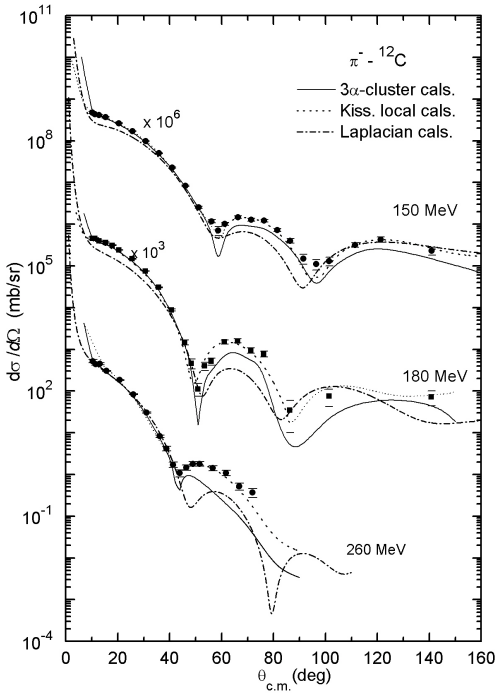

Fig. 1. Elastic scattering differential cross sections for 150, 180, and 260 MeV π^- on ^{12}C. The 3α-cluster model calculations use the solid curves, the Kisslinger local potential calculations use the dotted curves, and the Laplacian potential calculations use the dot-dashed curves. Solid points are the experimental data taken from Ref. [14].

π^--^{12}C complex Kisslinger local potential, Laplacian model, and 3α-cluster model are shown in Fig. 2 at 180 MeV. Both Kisslinger local potential and 3α-cluster model are attractive for real and imaginary potentials, where the Kisslinger local potentials are deeper and wider while those of α-particle model are shallower and sharper. For Laplacian model, the imaginary part is attractive while the real part is repulsive at smaller radii and attractive at large radii.

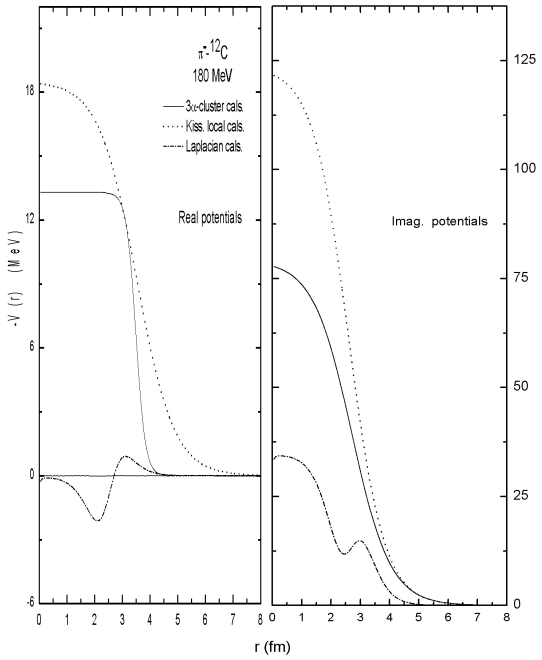

Fig. 2. Local optical potentials computed for 180 MeV π^- scattered from ^{12}C. The full curves are for the 3α-cluster potentials, the dotted curves for the Kisslinger local potential, and the dot-dashed curves for the Laplacian potentials. The left panel is for the real potential while the right is for the imaginary potential.

At lower pion beam energies $T_\pi < 100$ MeV, the elastic scattering differential cross sections of $\pi^\pm$ from ^{12}C at the pion kinetic energy 50 MeV are calculated using the three potential models. Most of these calculations show non-negligible difference between the prediction of the differential cross sections by the three potentials used here. We get a good agreement between the data and the Kisslinger local potential calculations when the second-order parameters are included beside the first-order parameters, as shown as dotted curves in Fig. 3 with χ^2=4.12 for π^+ and 3.44 for π^-. Calculations of the elastic scattering differential cross section based on Laplacian model, included the second order interaction parameters, shown as dot-dashed curves in Fig. 3 are in fairly agreement with data for both π^+ (χ^2=5.16) and π^- (χ^2=5.98). α-particle optical potential calculations do rather poorly than those of the other two considered potentials for both π^+ (χ^2=8.52) and π^- (χ^2=6.75).

Table II shows the χ^2 values calculated according to Eq. (6) for the three potential models considered here. At each pion energy, the χ^2 is minimum for Kisslinger-based local potential.

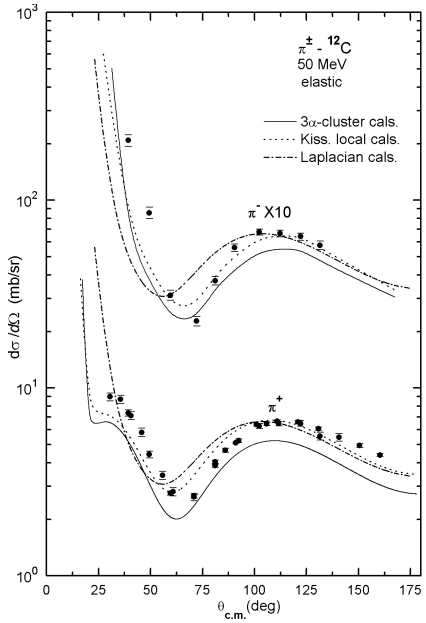

Fig. 3. As in Fig. 1 but for $\pi^{\pm}-^{12}$C elastic scattering differential cross sections at 50 MeV pion kinetic energy. The experimental data are taken from Ref. [15].

TABLE II

χ^2-values calculated in the present work according to Eq. (6) for $\pi^{\pm}$-^{12}C elastic scattering.

T_π (MeV)		3α-cluster cals. χ^2	$U_{\rm Loc}$ cals. χ^2	$U_{\rm Lap}$ cals. χ^2
50	π^+	8.52	4.12	5.16
50	π^-	6.75	3.44	5.98
150		9.13	2.80	10.41
180		11.22	3.47	13.62
260		11.65	4.63	14.12

As $k \longrightarrow 0$, the s-wave scattering length a_0=δ_0/k and p-wave scattering volume a_1=δ_1/k^3, where δ_0 and δ_1 are respectively the s- and p-wave phase shifts. Here a_0 and a_1 are calculated at 1 KeV for pions of both signs with the Coulomb potential omitted for the Kisslinger local and Laplacian potentials [18]. The magnitude of a is a measure of the strength of the interaction and its sign indicates whether the interaction is effectively repulsive or attractive.

The scattering lengths and volumes calculated from the two potentials are listed in Table III along with the values obtained from Ref. [18], and the experimental s-wave scattering lengths as tabulated by Hüfner [19]. Table III shows that magnitudes of a_0 and a_1 in the case of Kisslinger local potential are greater than those of Laplacian potential. The quantities of a_0 and a_1 calculated here are in a good agreement both in sign and magnitude with those of Refs. [18] and [19].

TABLE III

Zero-energy pion-^{12}C s-wave scattering lengths a_0 (fm) and p-wave scattering volumes a_1 (fm^3) calculated using the Kisslinger local and Laplacian potentials compared to other works.

	$U_{\rm Loc}$ cals.	$U_{\rm Lap}$ cals.	Exp. [19]	others [18]
Re a_0	-0.4398	-0.4021	-0.448	$-0.438 \longrightarrow -0.449$
Im a_0	0.1235	0.1182	0.132	$0.122 \longrightarrow 0.129$
Re a_1	1.8366	1.7815		$1.88 \longrightarrow 1.93$
Im a_1	0.4482	0.3517		$0.347 \longrightarrow 0.553$

Since inelastic scattering in the collective model is driven by the first derivative of the optical potential, agreement with such data can be a possible means to remove the ambiguity from elastic scattering fits. Here, angular distributions for the inelastic scattering of pions leading to the lowest 2^+ and 3^- states in ^{12}C are computed by the DWBA method using the zero-range code DWUCK4 due to Kunz [13]. The α-particle model optical potential may be tested, to predict observables of $\pi^{\pm}$ inelastically scattered from nuclei. A collective model distorted-wave Born approximation (DWBA) prediction using the three potential models considered in the present work shows that the Kisslinger local optical potential adequately fits the shape and magnitude of 50–260 MeV pion kinetic energies leading to the lowest 2^+ and 3^- states in ^{12}C as shown in Figs. 4–6. In the analysis presented here, the deformation lengths are varied until agreement is obtained with $\pi^{\pm}$ data.

Fig. 4 displays the predictions of the inelastic scattering differential cross sections of $\pi^{\pm}$ from ^{12}C nucleus excited to the lowest 2^+ state at 50 MeV. The inelastic data [15] are well represented by the present Kisslinger calculations with χ^2=1.82 for π^+ and 2.35 for π^- and Laplacian potential calculations with χ^2=4.28 for π^+ and 3.15 for π^-, when the first and second order parameters are included in both potentials, while calculations based on the 3α-particle model fail to agree with data at forward angles for π^+ with χ^2=9.13 and also give a poor fit with π^- data with χ^2=6.13.

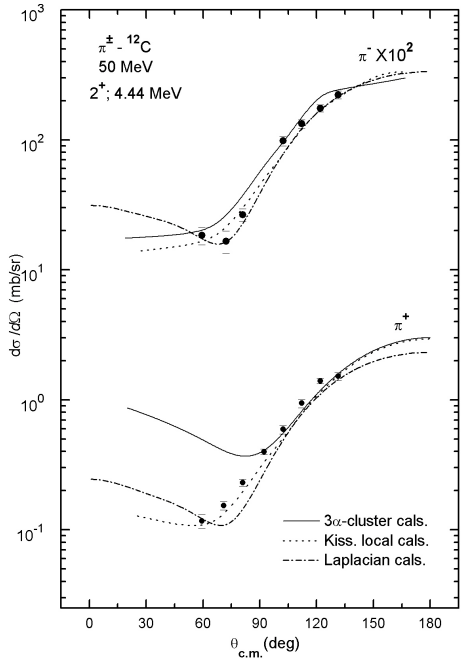

Fig. 4. As in Fig. 3 but for inelastic scattering differential cross sections of 50 MeV $\pi^{\pm}$ exciting the 4.44 MeV 2^+ state of ^{12}C. The experimental data are taken from Ref. [15].

Figs. 5 and 6 display the predictions of the inelastic scattering differential cross sections of π^- from ^{12}C nucleus excited to the lowest 2^+ and 3^- states at 150, 180, and 260 MeV. The three forms for the optical potential models give reasonable agreement with inelastic scattering data of Ref. [14], but the Kisslinger local potential predictions seem to be better at all energies considered in the present work with χ^2 ranging from 5.05–6.21 for 2^+ and 1.81–4.19 for 3^- states. These values of χ^2 are larger for Laplacian model (χ^2=6.35–8.16) for 2^+ and (χ^2=3.63–6.23) for 3^- states, while for α-particle model (χ^2=4.13–7.04) for 2^+ and (χ^2=2.18–4.23) for 3^- states except the case of 150 MeV π^- inelastic scattering.

From the above, we note that the fits reproduced on the basis of the α-cluster model of ^{12}C nucleus are more reasonable for low energy pions than for pions of higher energies. This is consistent with the conclusions of Li Qing-run [6]. This may indicate that the clustering phenomena in ^{12}C nucleus is more dominant for low pion energy scattering while pions of higher energies prefer to interact with ^{12}C nucleus as a whole. The predictions of the Kisslinger local potential well fit the data for differential cross sections at all energies under consideration.

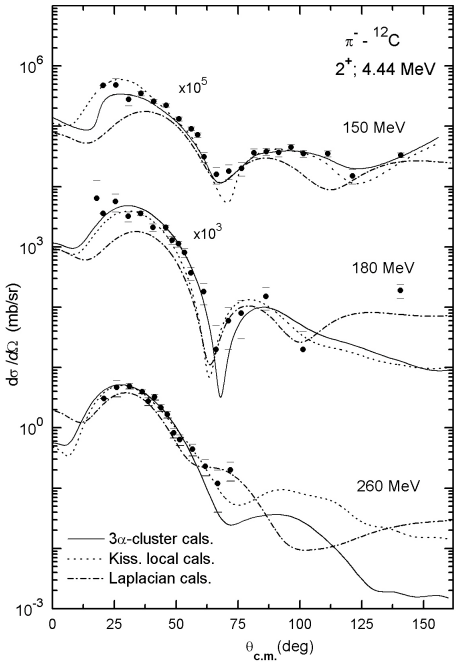

Fig. 5. As in Fig. 4, but for inelastic scattering differential cross sections of 150, 180, 260 MeV π^- exciting the 4.44 MeV 2^+ state of ^{12}C. The experimental data are taken from Ref. [14].

The values of the deformation lengths for all collective states analyzed here are summarized in Table IV and compared to those extracted from K^+ scattering [20] and to the corresponding ones previously extracted by others [21–24]. It is clear from Table IV that the deformation lengths of the real potential are greater than the corresponding ones for the imaginary potential in all cases under consideration. Real deformation lengths extracted here at 150 MeV for 2^+ and 180 MeV for 3^- are minimum. All values of deformation lengths extracted from the present work lie within or very close to the range of the corresponding values previously extracted from K^+ scattering and other particles on ^{12}C [20–24]. It can be seen from Table IV that the values of imaginary deformation lengths determined here using the 3α-particle model and Kisslinger local potential for 2^+ and 3^- excited states in ^{12}C increase with increasing pion kinetic energy, except for the case of 180 MeV π^- inelastic scattering off 3^- state in ^{12}C. This 180 MeV energy lies in the (3,3) resonance region of pions. Deformation length values extracted from the Kisslinger local and Laplacian potentials are higher than those extracted from the 3α-particle model, except for the imaginary deformation lengths

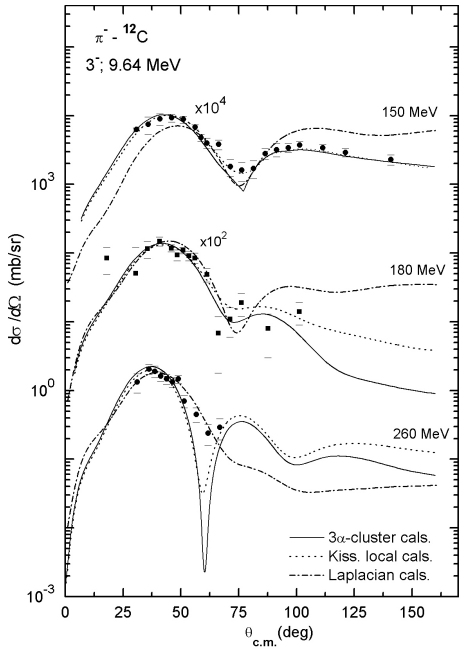

Fig. 6. As in Fig. 5, but for the 9.64 MeV 3^- state of ^{12}C.

for 180 and 260 MeV π^- off 2^+ state in ^{12}C using the Laplacian potential. Table IV also includes the calculated χ^2 values corresponding to each case under consideration. Again, it shows that χ^2 is minimum for the local Kisslinger potential at each of these cases except for π^- inelastic scattering of 150 MeV kinetic energy scattered to 2^+ and 3^- excited states in ^{12}C.

The DWUCK4 code using either of the three forms of potential considered here calculates the reaction cross sections σ_{R} of pion scattering from ^{12}C at pion kinetic energy ranging from 50 to 260 MeV. Following the same procedure the total cross sections σ_{T} are calculated here [20]:

$$\sigma_{\mathrm{T}} = \frac{2\pi}{k^2} \sum_L (2L + 1) \left[1 - \mathrm{Re}\, \eta_L\right], \tag{7}$$

where k is the incoming pion's wave number and η_L is the projectile–nucleus non-Coulomb amplitude. Table V shows the predicted σ_{R} and σ_{T} for pions of both signs scattering on ^{12}C at 50–260 MeV pion kinetic energy together with the corresponding cross sections estimated by others. The values of σ_{R} and σ_{T} predicted by these three potentials are found to be the same to within 1% regardless of the potential used but in most cases the local Kisslinger potential predictions are the nearest to the corresponding cross sections estimated by others. This result is not surprising in view of the

TABLE IV

Deformation lengths from $\pi^{\pm}$ inelastic scattering on ^{12}C calculated using the three potential methods considered in the present work compared to those extracted from K^+ inelastic scattering and other particles on ^{12}C [20–24]. The corresponding χ^2 values are also calculated.

T_π (MeV)	50	50	150	180	260	150	180	260
pion	π^+			π^-			π^-	
state				2^+			3^-	
3α-cluster model								
$\gamma_{\rm real}$ (fm)	1.511	1.401	1.315	1.418	1.531	1.207	1.138	1.196
$\gamma_{\rm imag}$ (fm)	1.113	1.082	1.121	1.145	1.214	0.936	0.907	1.103
χ^2	9.130	6.130	4.130	6.360	7.040	2.180	3.430	4.230
$U_{\rm Loc}$ model								
$\gamma_{\rm real}$ (fm)	1.514	1.412	1.405	1.517	1.604	1.273	1.212	1.277
$\gamma_{\rm imag}$ (fm)	1.213	1.103	1.207	1.243	1.316	1.025	0.982	1.112
χ^2	1.820	2.350	5.050	5.880	6.210	3.630	3.080	4.190
$U_{\rm Lap}$model								
$\gamma_{\rm real}$ (fm)	1.622	1.488	1.471	1.511	1.589	1.810	1.208	1.262
$\gamma_{\rm imag}$ (fm)	1.219	1.207	1.203	1.119	1.128	1.262	0.976	1.125
χ^2	4.280	3.150	6.350	9.490	8.160	1.115	5.440	6.230
K^+ scattering [20]								
$\gamma_{\rm real}$ (fm)				1.355–1.725			1.302–1.512	
$\gamma_{\rm imag}$ (fm)				0.978–1.114			0.955–1.214	
others								
γ (fm)	1.12–1.97		1.02–1.41	1.07 ± 0.05	1.50–1.21		0.65–1.23	
reaction	p–^{12}C		^{3}He–^{12}C	α–^{12}C	^{16}O–^{12}C		^{12}C–^{12}C	
	d–^{12}C						α–^{12}C	
	^{3}He–^{12}C						^{16}O–^{12}C	
References	[21]		[22]	[23]	[24]		[21]	

short mean-free path of pions in nuclei in this energy range which should make most of the scattering takes place in the nuclear surface. This is in contrast to the situation with low-energy pions. From Table V with the three forms of potential models, it is noticed for $\pi^{\pm}$ scattering of $T_\pi \geq 180$ MeV from ^{12}C that both calculated $\sigma_{\rm T}$ and $\sigma_{\rm R}$ decrease as the beam energy increases, and at all considered energies values of $\sigma_{\rm T}$ for π^- are greater than those for π^+ at a certain energy. This indicates that the mean free path λ for π^- is shorter than the corresponding λ for π^+. This is consistent with our previous results [12].

TABLE V

Total and Reaction cross sections in mb for $\pi^{\pm}$ scattering on ^{12}C calculated in the present work compared to other works.

T_π	pion	3α-cluster cals.		$U_{\rm Loc}$ cals.		$U_{\rm Lap}$ cals.		others		Ref.
		$\sigma_{\rm T}$	$\sigma_{\rm R}$	$\sigma_{\rm T}$	$\sigma_{\rm R}$	$\sigma_{\rm T}$	$\sigma_{\rm R}$	$\sigma_{\rm T}$	$\sigma_{\rm R}$	
(MeV)		(mb)	(mb)	(mb)	(mb)	(mb)	(mb)	(mb)	(mb)	
50	π^+	280.20	165.70	273.30	160.30	196.49	120.92	228.0	160.0	[18]
								248±20	152±14	[25]
180		590.00	388.00	570.00	380.00	641.66	422.26	581.0	384.0	[18]
220		532.30	322.54	530.36	313.72	550.51	336.62	521.0	318.0	[18]
50	π^-	302.10	190.80	292.70	189.15	258.74	153.19	290.0	200.0	[18]
150		703.30	467.63	683.50	442.80	703.25	467.63	696±7		[14]
180		675.03	439.97	666.20	424.10	675.33	439.25	615.0	400.0	[18]
								670±7		[14]
220		612.19	343.14	590.23	340.13	578.72	349.41	552.0	330.0	[18]
								586.0		[6]
260		499.10	325.40	529.40	315.60	487.62	277.27	536±6		[14]

4. Conclusion

Elastic, inelastic, total, and reaction cross sections are calculated using DWBA and the three forms of potential models, Kisslinger local, Laplacian, and the 3α-particle model formalisms. For the elastic scattering, there is a noticeable disagreement between the 3α-particle model calculations and data, especially at large angles in the region of (3,3) resonance; the data are larger than theory by a large factor. In the case of inelastic scattering, relatively little difference is seen between data and the α-particle model calculations. As the energy decreases the agreement with experiment gets better. We are able to obtain a good fit to the data for the elastic and inelastic scattering of 50–260 MeV pions from ^{12}C, using the Kisslinger local potential. The Kisslinger local potential calculations are much more comprehensive than α-particle model and Laplacian potential treatments, we may say that Johnson and Satchler emphasize a careful treatment of the first and second order optical potential. This potential includes also short-range correlations ζ. The second order parameters will be necessary to explain the data at lower pion energies < 100 MeV. The mean free path λ for π^- is shorter than the corresponding λ for π^+.

REFERENCES

[1] R.A. Eisenstein, G.A. Miller, *Comput. Phys. Commun.* **11**, 95 (1976).

[2] M.B. Johnson, *Phys. Rev.* **C22**, 192 (1980); M.B. Johnson, E.R. Siciliano, *Phys. Rev.* **C27**, 1647 (1983).

[3] K.M. Watson, *Phys. Rev.* **89**, 575 (1953).

[4] A.K. Kerman, H. McManus, R.M. Thaler, *Ann. Phys.* **8**, 551 (1959).

[5] R.H. Landau, A.W. Thomas, *Nucl. Phys.* **A302**, 461 (1978).

[6] Li Qing-run, *Nucl. Phys.* **A415**, 445 (1984).

[7] L.S. Kisslinger, *Phys. Rev.* **98**, 761 (1955).

[8] G. Fäldt, *Phys. Rev.* **C5**, 400 (1972).

[9] M.B. Johnson, G.R. Satchler, *Ann. Phys. (N. Y.)* **248**, 134 (1996).

[10] M. Krell, T.E.O. Ericson, *Nucl. Phys.* **B11**, 521 (1969).

[11] S.A.E. Khallaf, A.A. Ebrahim, *Phys. Rev.* **C62**, 024603 (2000).

[12] S.A.E. Khallaf, A.A. Ebrahim, *Phys. Rev.* **C65**, 064605 (2002).

[13] P.D. Kunz, DWBA code DWUCK4, University of Colorado, unpublished.

[14] F. Binon, P. Duteil, J.P. Garron, J. Gorres, L. Hugon, J.P. Peigneux, C. Schmit, M. Spighel, J.P. Stroot, *Nucl. Phys.* **B17**, 168 (1970).

[15] R.J. Sobie *et al.*, *Phys. Rev.* **C30**, 1612 (1984).

[16] A.A. Ebrahim, R.J. Peterson, *Phys. Rev.* **C54**, 2499 (1996).

[17] G.R. Satchler, *Nucl. Phys.* **A540**, 533 (1992).

[18] K. Stricker, H. McManus, J.A. Carr, *Phys. Rev.* **C19**, 929 (1979).

[19] J. Hüfner, *Phys. Rep.* **21C**, 1 (1975).

[20] A.A. Ebrahim, S.A.E. Khallaf, *Phys. Rev.* **C66**, 044614 (2002).

[21] S.M. Smith, G. Tibell, A.A. Cowley, D.A. Goldberg, H.G. Pugh, W. Reichart, N.S. Wall, *Nucl. Phys.* **A207**, 273 (1973) and references therein.

[22] A.S. Dem'yanova, E.F. Svinareva, S.A. Goncharov, S.N. Ershov, F.A. Gareev, G.S. Kazacha, A.A. Ogloblin, J.S. Vaagen, *Nucl. Phys.* **A542**, 208 (1992).

[23] M.E. Brandan, K.W. McVoy, *Phys. Rev.* **C43**, 1140 (1991).

[24] P.J. Moffa , C.B. Dover, J.P. Vary, *Phys. Rev.* **C16**, 1857 (1977).

[25] A. Saunders, S. Høibråten, J.J. Kraushaar, B.J. Kriss, R.J. Peterson, R.A. Ristinen, J.T. Brack, G. Hofman, E.F. Gibson, C.L. Morris, *Phys. Rev.* **C53**, 1745 (1996).